A Stereodivergent−Convergent Chiral Induction Mode in Atroposelective Access to Biaryls via Rhodium-Catalyzed C−H Bond Activation

Panjie Hu, Bingxian Liu, Fen Wang, Ruijie Mi, Xiao-Xi Li,* and Xingwei Li*
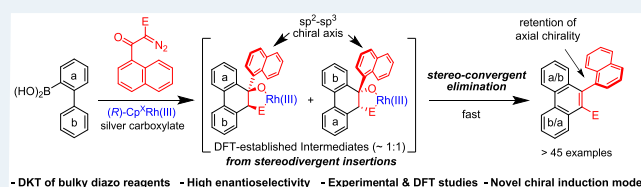
Read Online

ACCESS | Metrics & More | Article Recommendations | SI Supporting Information

ABSTRACT: Understanding the reaction mechanisms, particularly the chiral induction mode, is critical for the development of new asymmetric catalytic reactions. Rhodium(III)-catalyzed C−H activation en route to atroposelective [4 + 2] annulative coupling with α-diazo β-ketoesters has been realized, affording axially chiral phenanthrenes in good to excellent enantioselectivity. A combination of experimental and computational studies revealed a nontraditional stereodivergent−convergent chiral induction mode. The reaction proceeded with a rhodafluorene intermediate, followed by competitive, constructive, and stereodivergent migratory insertions of the two Rh−C(aryl) bonds into the carbene species to give β-ketoester intermediates. Then, the other Rh−C(aryl) bond migratorily inserts into the ketone carbonyl group. Following this stereodetermining carbonyl insertion, an ester-chelated rhodium(III) alkoxide species bearing two poorly controlled chiral centers and a well-controlled C(sp²)−C(sp³) chiral axis is generated. The final product is delivered via stereoconvergent elimination of a rhodium(III) species with retention of the well-controlled axial chirality and with loss of the central chirality.

KEYWORDS: enantioselective C−H activation, axial chirality, chiral induction mode, diazo reagent, annulation

INTRODUCTION

Asymmetric activation of C−H bond has been established as an increasingly important strategy toward the construction of chiral scaffolds.[1] Among various transition metals, palladium,[2] low- and high-valent cobalt/rhodium/iridium,[3] and nickel[4] catalysts are particularly powerful in delivering chiral products, especially atropoisomers.[5] In the last decade, as pioneered by Cramer[6] and further developed by You,[7] Waldmann,[8] Perekalin,[9] and Wang,[10] rhodium(III) catalysts stabilized by a chiral cyclopentadienyl ligand (Cp^X) have attracted increasing attention owing to their generality in asymmetric C(aryl)−H activation.[3] The effectiveness of Cp^XRh(III),[6−11] Cp^XIr(III),[12] Cp^XCo(III),[13] and related (η⁶-arene)Ru(II)[14] catalysts is ascribed to their unique stereoelectronic effect. As originally proposed by Cramer[6a,b] and further experimentally supported by our group,[11b,c] the chiral induction mode invariably involves initial recognition of the arene substrate by the chiral Cp^X ligand, leading to cyclometallation of the arene with a well-defined orientation (Scheme 1a).[15] The coupling partner is then dictated by the cyclometalated arene substrate. While this linear sequential substrate control mode proved very effective in diverse enantioselective C−H activation systems,[6,11] the challenges and limitations are also obvious. Both substrates need to be sterically and/or electronically biased to allow for initial and subsequent chiral recognition and to convey the chiral information throughout the catalytic process. In fact, low enantioselectivity was

observed for poorly distinguishable arene substrates or for unbiased metalacyclic intermediates.[11b,16]

On the other hand, asymmetric C−H activation systems may involve axial and central chirality in the intermediate or final product, where three relations exist between these two chiral elements. (1) The reaction may proceed with sequential, independent construction of both axial and central chirality.[3f,11g,17] (2) The reaction may give a centrally chiral intermediate, followed by chirality transfer to atroposelectively afford biaryls[8,17,18] or allenes[19] (Scheme 1b). (3) Occasionally, an axially chiral intermediate may undergo chirality transfer to give central chirality.[20] In all cases, the reactions require initial precise formation of a chiral center/axis.

To address the limitation of the predominant chiral induction mode and the limited relationship between multiple chiral elements, we conceived a new divergent−convergent chiral induction mode (Scheme 1c). Based on the same Cp^XRh(III) catalyst, the initial stereocenter-forming reaction does not have to be enantioselective. Instead, it generates one or more chiral centers with poor control. However, as long as a

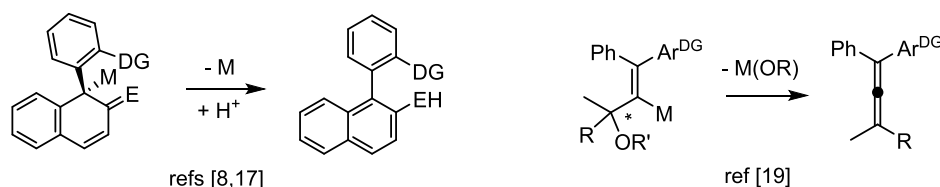**Scheme 1. Chiral Induction Mode in Asymmetric C−H Activation and Relationship Between Axial and Central Chirality**
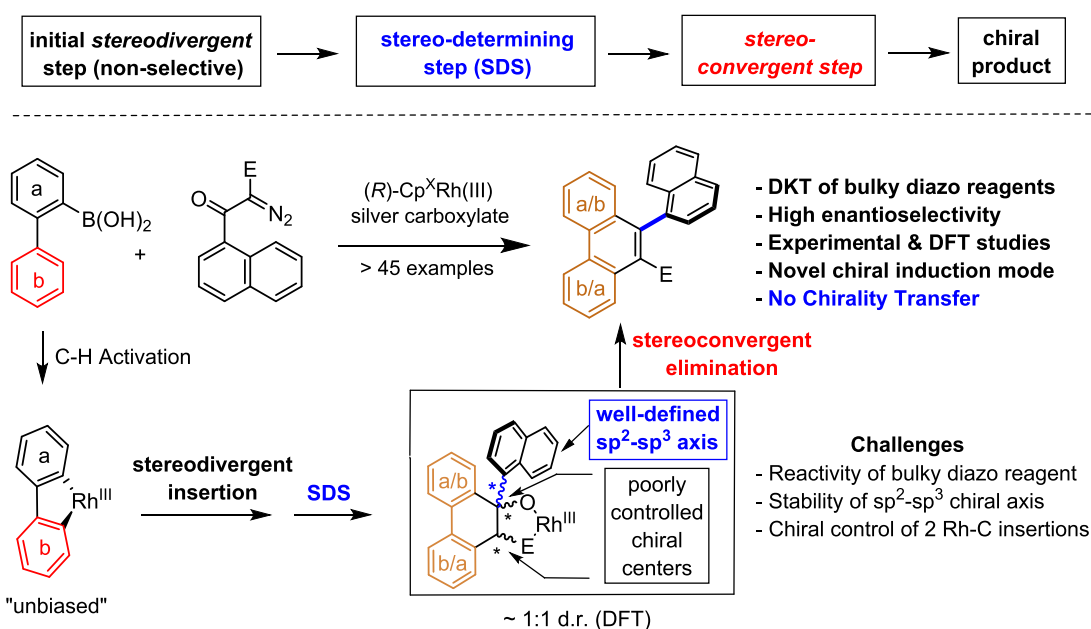

(a) **Linear chiral control mode in C-H Activation** (DG = directing group): **state of the art** [6a,b]
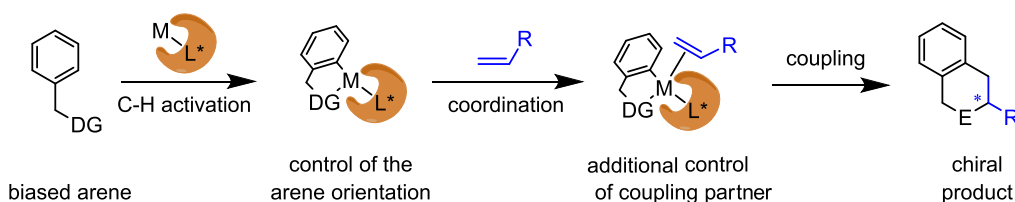
(b) **Asymmetric C-H Activation via Chirality Transfer** (*via* well-defined pre-existing or created chiral center)
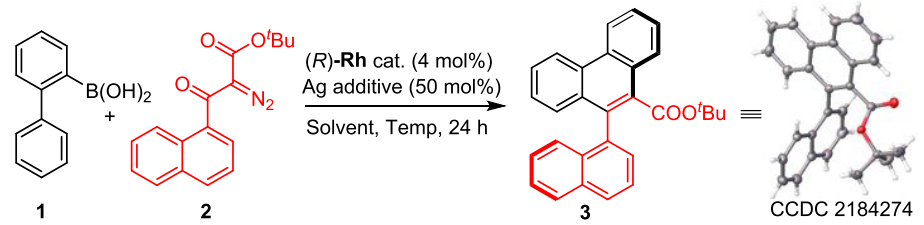
refs [8,17]   ref [19]

(c) **C-H Activation via Our Divergent-convergent Chiral Induction Mode** (*no chirality transfer*)
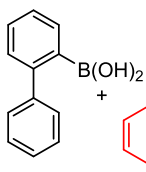
subsequent stereodetermining step exists, which creates a new chiral element with well-defined chirality, the multichirality intermediate may restore the chiral information and convey it to the final product, for example, by stereoconvergent removal of the chiral centers that were initially poorly controlled. Although the chiral information is partially lost from the intermediate to the final product, this novel divergent−convergent induction mode can effectively create a chiral element with more flexibility so that non-stereoselective steps may be accommodated and unbiased substrates can be employed. This mode stays in sharp contrast to chirality transfer because the central chirality in the intermediate is poorly controlled. Despite the design, this chiral induction mode requires a stereodetermining step to precisely build a chiral element that is not induced by the proximal (poorly controlled) chiral element.[21] In addition, the stereoconvergent transformation should effectively remove such poorly controlled chiral centers, while preserving the desired chiral element.
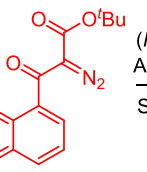
■ RESULTS AND DISCUSSION

Reaction Design. With this mode in mind, we set out to develop an atroposelective annulation system involving an intermediate with essentially indistinguishable bonds that may give rise to initial stereodivergence. We focused on annulation between a biphenyl-2-boronic acid[22] and a diazo[23] reagent by virtue of dynamic kinetic transformation of the latter (Scheme 1c). On note, although dynamic kinetic transformation of coupling reagents has been recently reported in C−H activation, these are restricted to sterically hindered alkynes.[11d,g,24] The most prominent feature of this system is the presence of a five-membered rhodafluorene intermediate containing two Rh−C bonds that are hardly distinguished by the chiral environment (Scheme 1c).[25] In this proof-of-concept study, the stereochemistry of the migratory insertion of two essentially indistinguishable Rh−C(aryl) bonds and the relationship between the insertion-derived multiple chiral elements constitute a divergent−convergent chiral induction

Table 1. Optimization Studies[a]

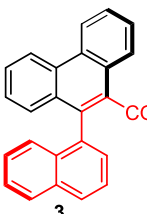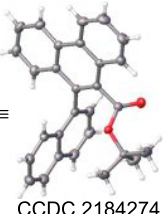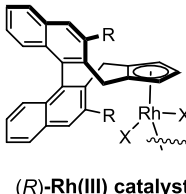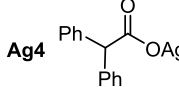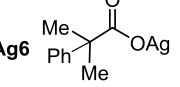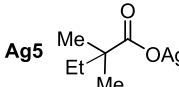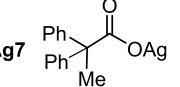| entry	cat.	additive	solvent	temp (°C)	ee (%)	yield (%)
1	Rh1	Ag1	THF	25	52	63
2	Rh1	Ag1	2-Me-THF	25	56	61
3	Rh2	Ag1	THF	25	86	65
4	Rh3	Ag1	THF	25	85	60
5	Rh4	Ag1	THF	25	84	63
6	Rh2	Ag1	^{t}BuOMe	25	90	59
7	Rh2	Ag1	2-Me-THF	25	92	62
8	Rh2	Ag2	2-Me-THF	25	92	50
9	Rh2	Ag3	2-Me-THF	25	90	71
10	Rh2	Ag4	2-Me-THF	25	92	68
11	Rh2	Ag5	2-Me-THF	25	91	49
12	Rh2	Ag6	2-Me-THF	25	91	57
13	Rh2	Ag7	2-Me-THF	25	91	45
14	**Rh2**	**Ag4**	**2-Me-THF**	**30**	**91**	**82**
15	Rh2	Ag4	2-Me-THF	40	88	82
16	Rh3	Ag4	2-Me-THF	30	86	35
17	Rh3	Ag4	^{t}BuOMe	30	86	61
18	Rh3	Ag1	^{t}BuOMe	30	87	71
19	Rh3	Ag2	^{t}BuOMe	30	86	64
20	Rh3	Ag3	^{t}BuOMe	30	86	70
21	Rh3	Ag5	^{t}BuOMe	30	84	65
22	Rh3	Ag6	^{t}BuOMe	30	85	67
23	**Rh3**	**Ag7**	**^{t}BuOMe**	**30**	**88**	**75**
24	Rh4	Ag4	2-Me-THF	30	84	63
25	Rh4	Ag7	^{t}BuOMe	30	86	77

[a]Reaction conditions: **1** (0.05 mmol), **2** (0.075 mmol), (R)-**Rh** (4 mol %), **Ag** (50 mol %) in the solvent (1 mL), 24 h, isolated yield. The ee was determined by HPLC using a chiral stationary phase.

scenario. However, the formation and retention of a well-defined, relatively stereochemically labile C(sp^2)−C(sp^3)[26] chiral axis poses a big challenge. Of note, this working mode differs from that in recently reported nickel-catalyzed stereoconvergent C−C coupling using racemic alkyl halides because no initial stereodivergence is involved.[27] Our system also drastically differs from the well-explored central-to-axial[8,18] chirality transfer systems because a well-defined central chirality would be a prerequisite. We now report our experimental and theoretical studies on atroposelective synthesis of phenanthrenes.

Optimization Studies. We initially carried out optimization studies using biphenyl-2-boronic acid (**1a**) and an acceptor−acceptor diazo reagent (**2a**) as the substrates (Table 1). The desired annulation reaction occurred in the presence of the Cramer-type (R)-**Rh1** catalyst and AgOAc as

an additive in a variety of ethereal solvents, and product **3** was obtained in moderate yield and promising enantioselectivity (Table 1, entries 1 and 2). Significantly higher enantioselectivity was reached when a small set of chiral catalysts (R)-**Rh2**−**Rh4** bearing different side arms were employed,[6b,c,12a,28] and the enantioselectivity varied within a small range. Since the (R)-**Rh2** catalyst slightly outperformed the rest in enantioselectivity, it was retained for further optimization. It was found that different silver additives only had insignificant influence on the enantioselectivity in the 2-Me-THF solvent. Nevertheless, the employment of **Ag4** as an additive afforded high yield and excellent enantioselectivity and 30 °C seemed to be the optimal reaction temperature (entry 14, denoted as Conditions A). The absolute configuration of product **3** was established to be (S) by X-ray crystallography (CCDC 2184274). As a backup, further studies revealed that a combination of (R)-**Rh3**
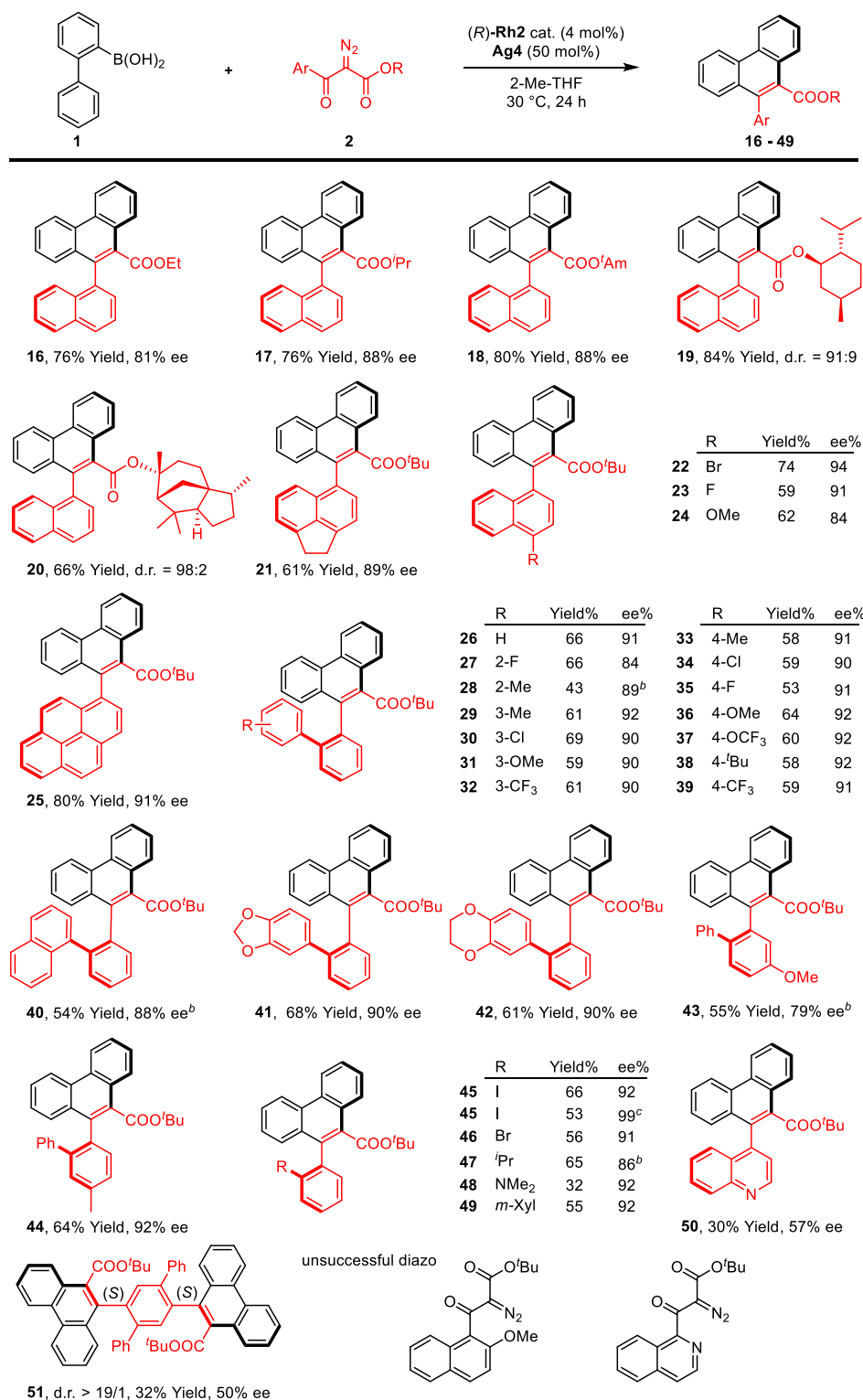
Scheme 2. Scope of Biphenyl Boronic Acid in [4 + 2] Annulation[a]
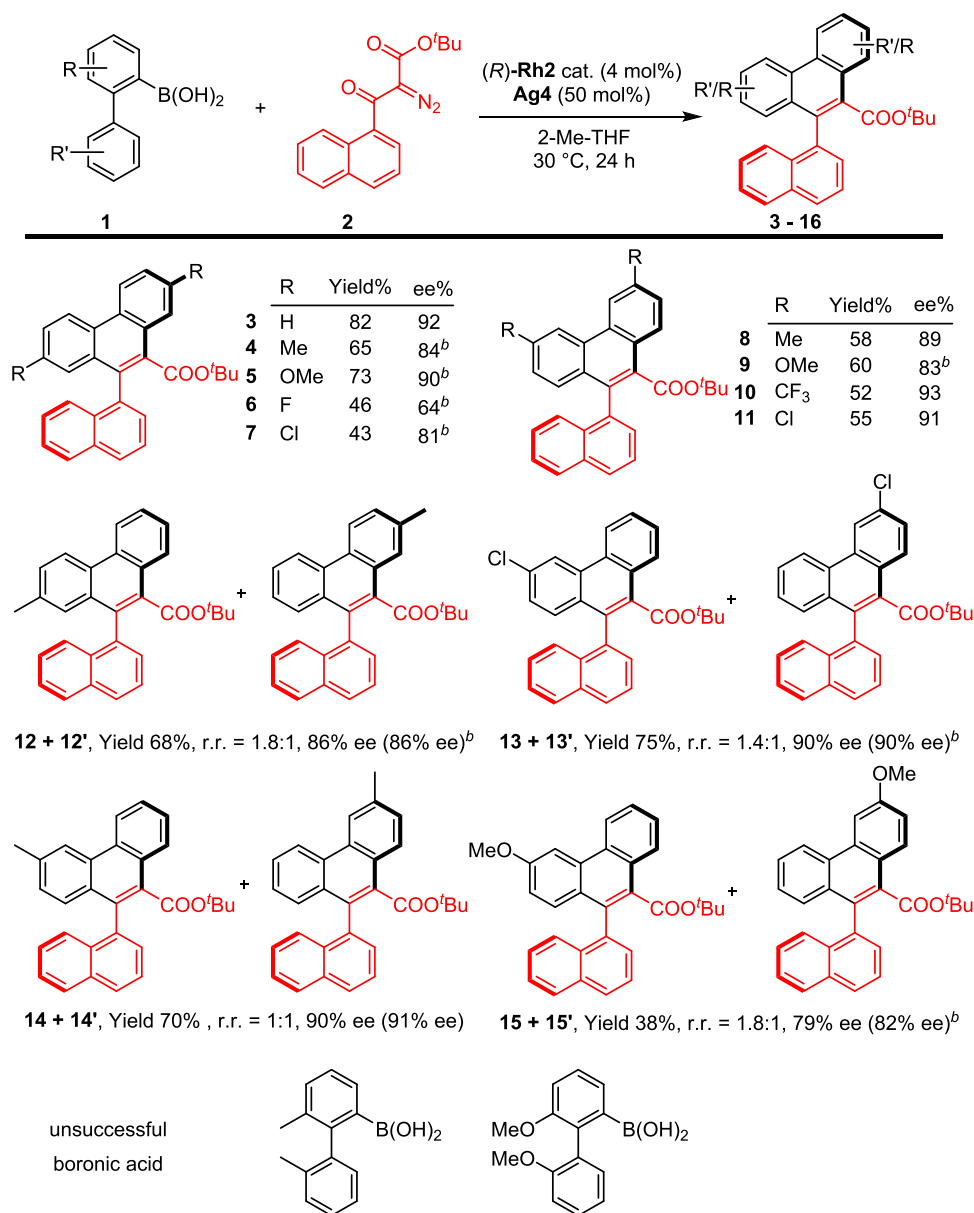
	R	Yield%	ee%
3	H	82	92
4	Me	65	84[b]
5	OMe	73	90[b]
6	F	46	64[b]
7	Cl	43	81[b]

	R	Yield%	ee%
8	Me	58	89
9	OMe	60	83[b]
10	CF₃	52	93
11	Cl	55	91

12 + 12', Yield 68%, r.r. = 1.8:1, 86% ee (86% ee)[b]   **13 + 13'**, Yield 75%, r.r. = 1.4:1, 90% ee (90% ee)[b]

14 + 14', Yield 70%, r.r. = 1:1, 90% ee (91% ee)   **15 + 15'**, Yield 38%, r.r. = 1.8:1, 79% ee (82% ee)[b]

unsuccessful boronic acid

[a]Reaction conditions: **1** (0.1 mmol), **2** (0.15 mmol), (*R*)-**Rh2** (4 mol %), **Ag4** (50 mol %) in 2-Me-THF (2 mL), 24 h, 30 °C. [b]Reaction conditions: **1** (0.1 mmol), **2** (0.15 mmol), (*R*)-**Rh3** (4 mol %), **Ag7** (50 mol %) in ᵗBuOMe (2 mL), 24 h, 30 °C. Isolated yield. The ee was determined by HPLC using a chiral stationary phase.

catalyst and **Ag7** in ᵗBuOMe solvent also formed suitable reaction conditions, which afforded product **3** in 88% ee and 75% yield (Conditions B). The (*R*)-**Rh4** catalyst delivered slightly inferior results under various reaction conditions. Previously, asymmetric C−H activation−annulation systems have been mostly limited to the synthesis of heteroarenes with alkynes and olefins being predominantly used as C2 synthons, while diazo reagents were predominantly used as C1 synthons.[20,29]

Reaction Scope. The scope and limitation of this atroposelective annulation system was next studied (Scheme 2). The coupling of different disubstituted boronic acids leading to symmetric products was examined first. Boronic acid bearing different substituents at the *para* positions were found to react under Conditions B with enantioselectivity superior to that under Conditions A (**4−7**), where noticeable steric and/

or electronic effect of the substituent was detected. The enantioselectivity was generally high, and an electron-withdrawing group tends to give attenuated enantioselectivity (**6** and **7**). Very limited influence was observed when both electron-donating (Me and OMe) and electron-withdrawing (Cl and CF₃) groups were introduced into the *meta* position, and all of the products were isolated in high to excellent enantioselectivity (**8−11**). The scope of boronic acids that lead to unsymmetric annulation products was also explored. Boronic acids bearing a methyl group at the *para* or *meta* position afforded two regioisomeric products in poor rr (**12**/**12′** and **14**/**14′**). The introduction of a *meta* chloro group was also tolerated, affording two products in excellent enantioselectivity and in 1.4:1 rr (**13**/**13′**). Slightly lower reactivity and enantioselectivity was observed when a *meta* methoxy group was present (**15**/**15′**), indicative of the weak electronic effect.

Scheme 3. Scope of Diazo Reagent in [4 + 2] Annulation[a]

	R	Yield%	ee%
22	Br	74	94
23	F	59	91
24	OMe	62	84

	R	Yield%	ee%		R	Yield%	ee%
26	H	66	91	33	4-Me	58	91
27	2-F	66	84	34	4-Cl	59	90
28	2-Me	43	89[b]	35	4-F	53	91
29	3-Me	61	92	36	4-OMe	64	92
30	3-Cl	69	90	37	4-OCF$_3$	60	92
31	3-OMe	59	90	38	4-^{t}Bu	58	92
32	3-CF$_3$	61	90	39	4-CF$_3$	59	91

	R	Yield%	ee%
45	I	66	92
45	I	53	99[c]
46	Br	56	91
47	^{i}Pr	65	86[b]
48	NMe$_2$	32	92
49	m-Xyl	55	92

16, 76% Yield, 81% ee　　**17**, 76% Yield, 88% ee　　**18**, 80% Yield, 88% ee　　**19**, 84% Yield, d.r. = 91:9

20, 66% Yield, d.r. = 98:2　　**21**, 61% Yield, 89% ee

25, 80% Yield, 91% ee

40, 54% Yield, 88% ee[b]　　**41**, 68% Yield, 90% ee　　**42**, 61% Yield, 90% ee　　**43**, 55% Yield, 79% ee[b]

44, 64% Yield, 92% ee　　　　　　　　　　**50**, 30% Yield, 57% ee

51, d.r. > 19/1, 32% Yield, 50% ee

unsuccessful diazo

[a]Reaction conditions: **1** (0.1 mmol), **2** (0.15 mmol), (R)-**Rh2** (4 mol %), **Ag4** (50 mol %) in 2-Me-THF (2 mL), 24 h, 30 °C. [b]Reaction conditions: **1** (0.1 mmol), **2** (0.15 mmol), (R)-**Rh3** (4 mol %), **Ag7** (50 mol %) in ^{t}BuOMe (2 mL), 24 h, 30 °C. isolated yield. The ee was determined by HPLC using a chiral stationary phase. [c]After recrystallization.

In all cases, both regioisomeric products were obtained in nearly the same enantioselectivity in each specific reaction and the rr only varied within a small range.

The scope of the diazo reagent was next examined under reaction Conditions A or B (Scheme 3). Variation of the ester group to ^{t}Amyl, Et, and ^{i}Pr esters all gave satisfying enantioselectivity and reaction efficiency (**16–18**, 81–88% ee), where the enantioselectivity of the product seems correlated to the steric effect of the ester group. The reaction is also compatible with natural product-derived diazo reagents.

Scheme 4. Synthetic Applications of Selected Products
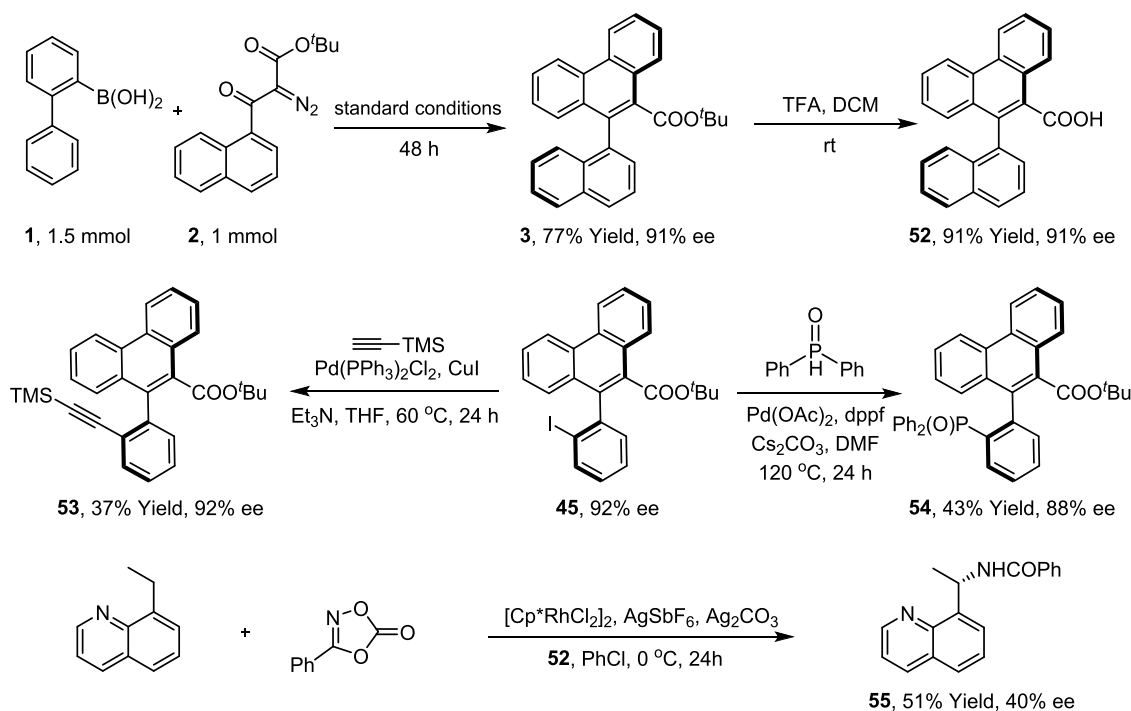
In line with the above observed stereoselectivity, the menthol ester coupled to give product **19** in 91:9 dr, while excellent diastereoselectivity (dr = 98:2) was observed when cedrol, a tertiary alcohol, was installed (**20**). The 1-naphthyl group in the diazo reagent was successfully extended to several substituted ones bearing electron-donating and electron-withdrawing groups (**21−24**) and to a fused aryl group (**25**). The 1-naphthyl group that defines the axial chirality was further extended to diverse classes of *ortho*-substituted bulky aryl groups (**26−49**). Thus, biphenyl groups bearing a diverse array of electron-donating, electron-withdrawing, and halogen groups at the *ortho*, *meta*, and *para* positions of one of the phenyl rings all reacted in excellent enantioselectivity (**26−44** and **49**, 84−92% ee). In addition to biphenyl groups, the bulky aryl ring can be expanded to those bearing other useful *ortho* functional groups such as alkyl, halo, and dimethylamino groups (**45−48**). In addition, the diazo reagents with either a heterocycle or two prochiral axis only reacted to deliver the corresponding product with a low yield and moderate enantioselectivity (**50** and **51**). Unexpectedly, the 2-substituted naphthyl ring in the diazo reagents were incompatible with our standard conditions. In all cases, variable amounts of biphenyl were detected as a byproduct as a result of protodeboronation. The atropostability of a representative product **3** has been analyzed, and essentially no decay of enantiopurity was detected when heated at 100 °C (PhCl). This corresponds to a racemization activation free energy of $\Delta G^{\neq}$ >34 kcal/mol.

Synthetic Applications. Synthetic applications of representative products were next demonstrated. The reaction of **1** and diazo reagent **2** was scaled up to a 1 mmol scale from which product **3** was isolated in good yield with no deterioration of enantioselectivity (Scheme 4). Treatment of product **3** with TFA afforded chiral acid **52** in high yield. Product **45** with an *ortho* iodo group underwent smooth Pd-catalyzed coupling with diphenylphosphine oxide to afford the phosphorylated product **54** in acceptable yield. The Sonoga-

shira coupling between **45** and trimethylsilylacetylene afforded product **53** in moderate yield. In all cases, only slight or no erosion of enantiopurity was observed during the transformations. Chiral acid **52** was further applied as an additive in the Cp*Rh(III)-catalyzed enantioselective amidation of a methylene group.[30] Our initial studies using 8-ethylquinoline afforded the amidated product **55** in 40% ee, indicating potentiality of this acid in asymmetric catalysis.

Mechanistic Studies. A series of experimental studies were conducted to probe the reaction mechanism. The coupling of **1** and **2** was carried out under modified standard conditions A with extra D_2O (3 equiv). NMR analysis of the product revealed slight H/D exchange at two *ortho* positions (Scheme 5a), suggesting reversibility of rollover C−H activation/cyclometalation during the formation of the rhodafluorene intermediate. Kinetic isotope effect was then determined by parallel reactions using **1** or **1**-d_5 under modified reaction conditions with low conversions, and ^{1}H NMR analysis revealed an estimated value of KIE = 1.5 (Scheme 5b), suggesting that the C−H activation event is not involved in the turnover-limiting step. To further explore the mechanistic details, a stoichiometric reaction between boronic acid **1** and (*R*)-**Rh1** was conducted in the presence of a σ donor (pyridine),[22c,31] affording rhodafluorene **56** as the sole organorhodium species (Scheme 5c). Designation of **56** as a catalyst for the coupling of **1** and **2** afforded product **3** in essentially the same enantioselectivity (60%) as that obtained from the catalytic reaction (Table 1, entry 2). In addition, the stoichiometric reaction of a *para*-methyl substituted boronic acid (**1j**) with (*R*)-**Rh1** afforded a diastereomeric mixture of complexes **57** and **57′** in 1:1 diastereomeric ratio as determined by NMR analysis (Scheme 5e). This observation indicates that the arene substrate undergoes transmetalation−cyclometalation with poor control of the initial orientation of the arene. The 1:1 ratio of stoichiometric products **57** and **57′** is also consistent with 1:1 regioselectivity of the products

Scheme 5. Mechanistic Studies
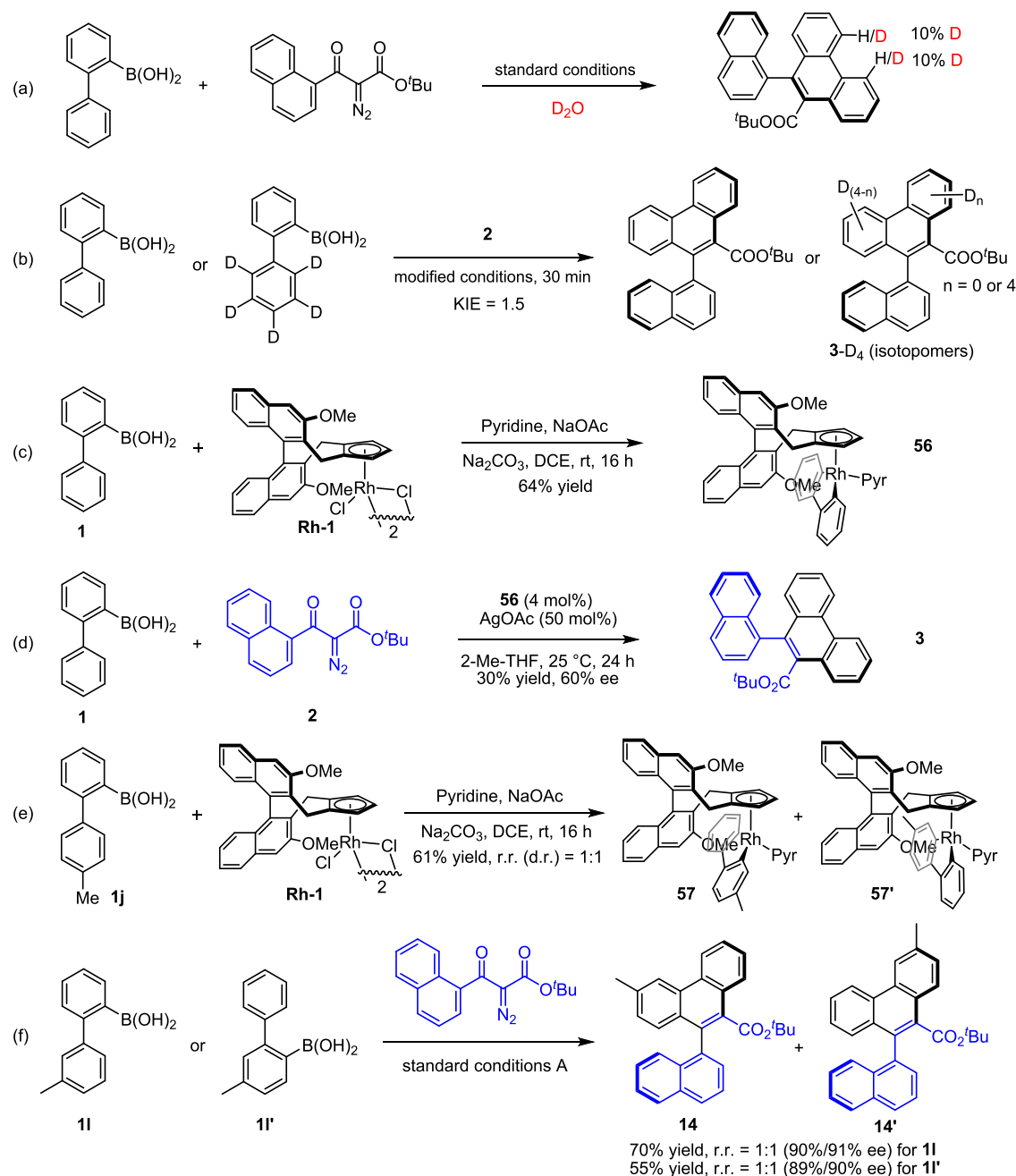
generated from the catalytic reaction using the (R)-**Rh1** precatalyst (see the Supporting Information). This conclusion was further supported by regioconvergent coupling reactions using different arylboronic acids **1l** and **1l′**. Thus, the reaction of either **1l** or **1l′** with diazo reagent **2** afforded the same product mixture (**14** and **14′**) in 1:1 regioselectivity, and each regioisomer was produced in essentially the same enantioselectivity (89−91% ee) although the reaction efficiency slightly varied (Scheme 5f). These data validated that these two substrates reacted via the same rhodafluorene intermediate, and the kinetic profile defined by the sequential migratory insertions of both Rh−C(aryl) bonds is essentially duplicated. Mechanistically, the regioselectivity of the insertion of the two Rh−C bonds dictates the regioselectivity of the final product, and the two Rh−C(aryl) bonds in rhodafluorene intermediates

56 and **57**/**57′** are essentially kinetically indistinguishable, which should accordingly afford the corresponding alkylation intermediate in poor initial stereoselectivity (vide infra). Clearly, our coupling system worked against the linear chiral induction mode depicted in Scheme 1a.

Summary of Competing Pathways. To elucidate the origins of enantioselectivity and the relationship between the axial and temporary central chirality, we have conducted mechanistic studies by DFT methods.[32] The DFT-computed two competing and constructive pathways are summarized in Scheme 6. Starting from the rhodacyclic intermediate **Int1**, each of the Rh−C bonds in **Int1** may undergo competitive migratory insertion into the carbene to give **Int2** or **Int2**§ following protonolysis (by AcOH). Then, the second migratory insertion occurs to give the Rh(III) alkoxide

Scheme 6. Summary of Two Competing and Constructive Pathways That Afford the (Same or Regioisomeric) Observed Enantiomeric Product
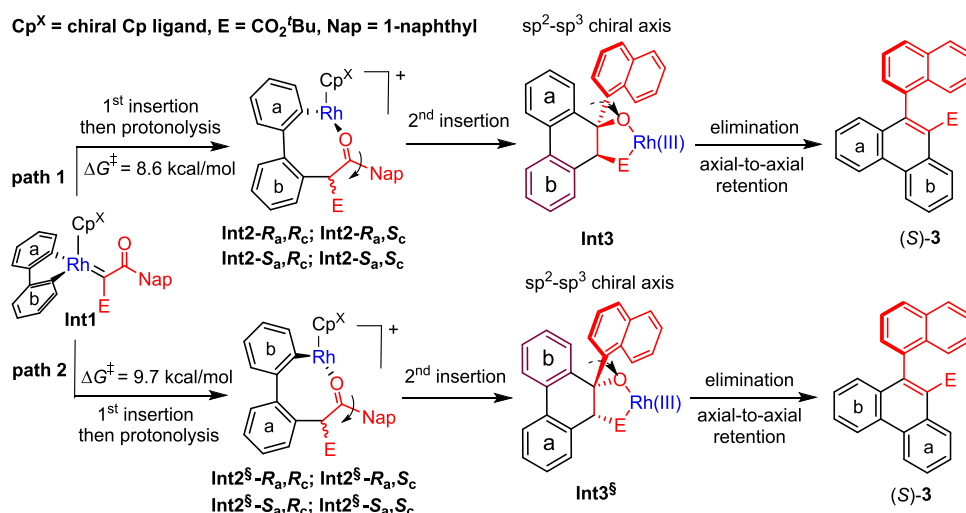
Scheme 7. Free-Energy Profiles Including D3BJ Corrections (in kcal/mol) of the Second Rh−C Migratory Insertion and the Subsequent Elimination Calculated at the B3LYP/Def2TZVPP//Def2SVP(PCM) Level for Path 1
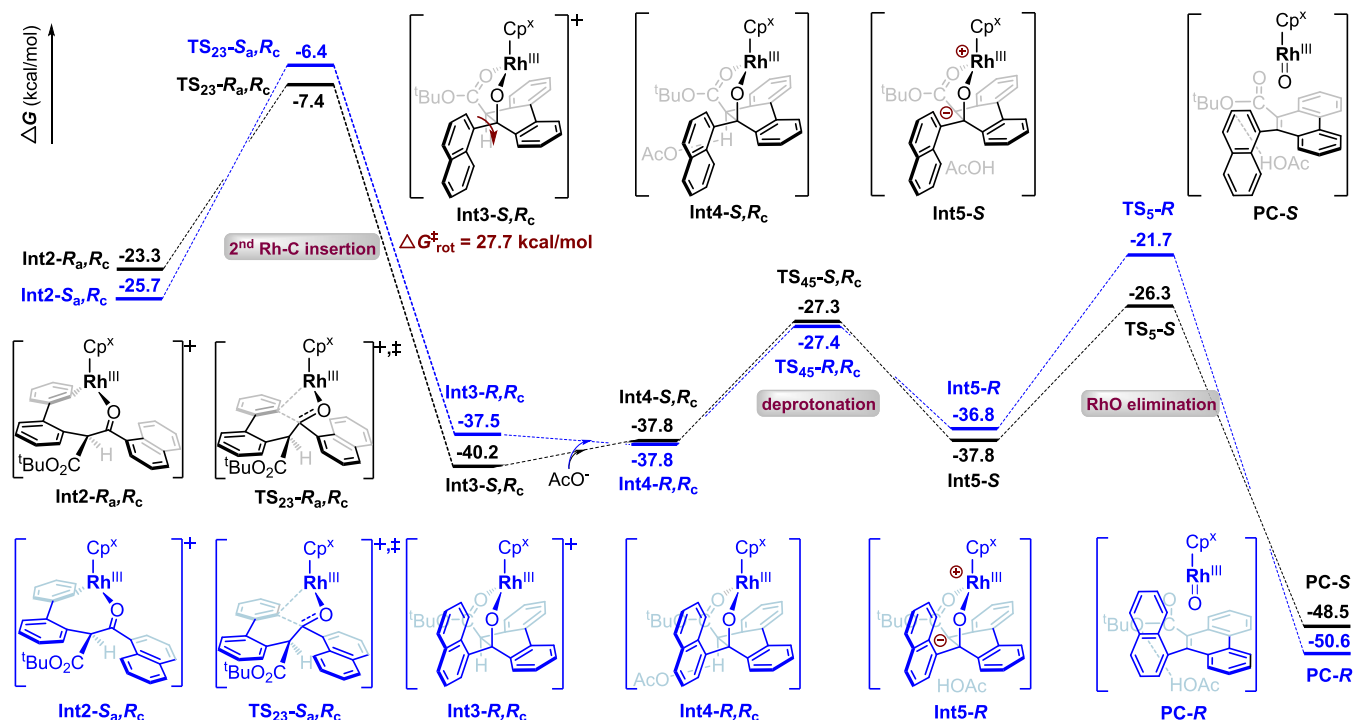
intermediate **Int3** or **Int3§**. Subsequent stereoconvergent elimination of the Rh(III) oxide furnishes the final product.

Insertion Process of Path 1. In Path 1 that is defined by initial migratory insertion of the b-aryl group in **Int1**, this migratory insertion was calculated to bear an activation barrier of 8.6 kcal/mol, and the subsequent protonolysis afforded four diastereomeric rhodium aryl-ketone intermediates **Int2-R_a,R_c**, **Int2-R_a, S_c**, **Int2-S_a, R_c**, and **Int2-S_a,S_c** as a combination of the central chirality and the prochiral C(O)−Nap axis (Scheme S1).[33] Since the β-ketoester moiety is readily enolizable, the chiral center in the **Int2** set may carry no meaningful information per se, but it affects the subsequent second migratory insertion. The two (R)-centrally configured intermediates (**Int2-R_a,R_c** and **Int2-S_a,R_c**) all insert irreversibly

with a lower activation barrier due to a reduced steric effect (Schemes 7 and S2). Consequently, the energies of the transition states **TS$_{23}$-R_a,R_c** (−7.4 kcal/mol) and **TS$_{23}$-S_a,R_c** (−6.4 kcal/mol) are lower than those of the other two that correspond to the insertion of the two (S)-configured intermediates (**Int2-R_a,S_c** and **Int2-S_a,S_c**, Scheme S2). Thus, the two lowest-lying transition states were found to have a $\Delta\Delta G^{\ddagger}$ of 1.0 kcal/mol, favoring the formation of rhodium ester-alkoxide **Int3-S,R_c** that eventually leads to the observed (S) product (vide infra). Of note, the alternative migratory insertion of the corresponding acetate-bound, 18-electron Rh(III) species proceeds through a transition state that is 7.0 kcal/mol higher than the energy of **TS$_{23}$-R_a,R_c** (Scheme S3). Therefore, the migratory insertion of such an 18-electron

species can be safely ruled out, which is consistent with negligible variation of enantioselectivity when diverse silver carboxylate additives were used (Table 1). Of note, the most prominent feature of the rhodium ester-alkoxide **Int3-S,R$_c$** is the presence of an atropomerically stable $C(sp^3)-C(1-$naphthyl) chiral axis with the kinetic barrier of rotation–epimerization being calculated to be as high as 27.7 kcal/mol.

Elimination Mechanism. The subsequent elimination in Path 1 was examined for both alkoxide intermediates **Int3-S,R$_c$** and **Int3-R,R$_c$** and was found to follow an E1cb mechanism[34] via carboanions **Int5-S** and **Int5-R**, respectively (Scheme 7). The overall barriers of E1cb for the generation of the (S) product and (R) product are 11.5 and 16.1 kcal/mol, respectively, which are much lower than the epimerization barrier (27.7 kcal/mol) of the chiral axis in **Int3-S,R$_c$**. Our attempts to locate the transition states of other possible elimination pathways (E1 and E2) all failed, likely due to the high acidity of α-proton induced by the proximal ester. The rapid elimination and the calculated atropostability of the $C(sp^2)-C(sp^3)$ chiral axis support the conclusion that the second migratory insertion is stereodetermining. Our observations of axial-to-axial retention stay in contrast to the extensively explored point-to-axial chirality transfer[17] because the central chirality in the intermediate was poorly controlled due to stereodivergence.

Establishment of Two Competing Pathways. Meanwhile, we identified the energy profile of the competing Path 2 (Table 2 and Scheme S1). The initial migratory insertion was

Table 2. Summary of the Relative Energies (in kcal/mol) of Key Transition States in Two Parallel Pathways[a]

	1st Insertion (Scheme S1)	2nd Insertion (stereo-determining) (Scheme S2)	
		(S)-forming **TS**	(R)-forming **TS**
Path 1	8.6 **TS$_1$**	-7.4 **TS$_{23}$-R$_a$,R$_c$**	-6.4 **TS$_{23}$-S$_a$,R$_c$**
Path 2	9.7 **TS$_1$§**	-6.9 **TS$_{23}$§-R$_a$,S$_c$**	-4.5 **TS$_{23}$§-S$_a$,S$_c$**

[a]The rhodacyclic carbene intermediate **Int1** is set to zero energy.

found to bear an activation free energy of 9.7 kcal/mol, which is closely comparable to that in Path 1 (8.6 kcal/mol). In line with the findings of the insertion in Path 1, the two lowest-lying transition states **TS$_{23}$§-R$_a$,S$_c$** (−6.9 kcal/mol) and **TS$_{23}$§-S$_a$,S$_c$** (−4.5 kcal/mol) were identified for the insertion of two (S)-centrally configured ketone intermediates (**Int2§-R$_a$,S$_c$** and **Int2§-S$_a$,S$_c$**), respectively (Scheme S2). The $\Delta\Delta G^{\neq}$ of this second migratory insertion was found to be 2.4 kcal/mol, also favoring the formation of the same (S) product upon rapid

elimination. The key transition states in the kinetic profiles are summarized in Table 2 for both pathways. Analysis of the transition states (**TS$_{23}$-R$_a$,R$_c$** and **TS$_{23}$-S$_a$,R$_c$**) in Path 1 indicated that the steric repulsion between the naphthyl ring and the cyclopentadienyl ring raised the energy of the latter, while the energy difference between **TS$_{23}$§-S$_a$,S$_c$** and **TS$_{23}$§-R$_a$,S$_c$** in Path 2 is due to the steric repulsion between the naphthyl ring and the aryl group (Scheme S4). These data validated that the energy profiles of the two competing pathways essentially mirror each other. Collectively, Paths 1 and 2 contribute 73 and 27%, respectively, to the product formation. Based on the weight-averaged enantioselectivity of each pathway, an overall 90% ee was calculated, which agrees with our experimental observations. These calculated energy profiles are also in accordance with the poor regioselectivity of related products (12−15), supporting our proposal of our divergent−convergent chiral induction mode.

CONCLUSIONS

We have realized atroposelective C−H activation of biphenyl-2-boronic acids and annulation with diazo reagents. Our experimental studies indicated that the coupling system proceeded through a C−H bond activation pathway to give a five-membered rhodafluorene intermediate in which the two Rh−C(aryl) bonds are nearly kinetically indistinguishable toward the subsequent migratory insertion. Detailed mechanistic profile has been further elucidated by DFT studies, and the two Rh−C bonds undergo competitive migratory insertion to afford a β-ketoester moiety. Then, a second stereo-determining migratory insertion of the other Rh−C(aryl) bond occurs into the ketone carbonyl group, affording an ester-stabilized rhodium(III) alkoxide species bearing two poorly controlled chiral centers but with a proximal $C(sp^2)-C(sp^3)$ chiral axis that is precisely controlled. The final product is delivered upon rapid stereoconvergent elimination of a rhodium(III) species with retention of the axial chirality and with loss of the central chirality. This stereodivergent−convergent mode of chiral induction stays in contrast to the predominant linear chiral induction mode or the point-to-axial chirality transfer process, and it constitutes a rare working mode in asymmetric catalysis. We anticipate that this mode will inspire further discovery of related enantioselective C−H activation and other asymmetric catalytic systems. Future studies of other atroposelective catalytic systems are underway in our laboratories.

ASSOCIATED CONTENT
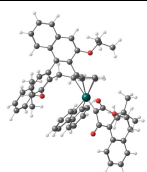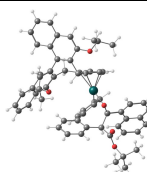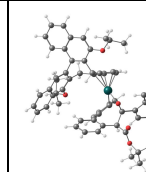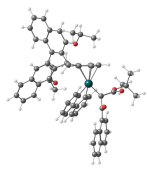
Supporting Information
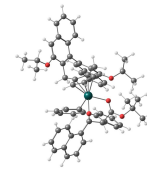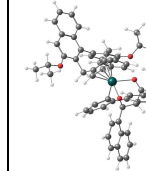
The Supporting Information is available free of charge at https://pubs.acs.org/doi/10.1021/acscatal.2c04292.

Detailed experimental procedures, characterization data, and NMR spectra of new compounds (PDF)

Accession Codes

■ AUTHOR INFORMATION

Corresponding Authors

Xiao-Xi Li − *Institute of Molecular Sciences and Engineering, Institute of Frontier and Interdisciplinary Science, Shandong University, Qingdao 266237, China;* orcid.org/0000-0002-3593-7536; Email: lixiaoxi@sdu.edu.cn

Xingwei Li − *School of Chemistry and Chemical Engineering, Shaanxi Normal University, Xi'an 710062, China; Institute of Molecular Sciences and Engineering, Institute of Frontier and Interdisciplinary Science, Shandong University, Qingdao 266237, China;* orcid.org/0000-0002-1153-1558; Email: lixw@snnu.edu.cn

Authors

Panjie Hu − *School of Chemistry and Chemical Engineering, Shaanxi Normal University, Xi'an 710062, China*

Bingxian Liu − *School of Chemistry and Chemical Engineering, Henan Normal University, Xinxiang 453007, China*

Fen Wang − *School of Chemistry and Chemical Engineering, Shaanxi Normal University, Xi'an 710062, China*

Ruijie Mi − *Institute of Molecular Sciences and Engineering, Institute of Frontier and Interdisciplinary Science, Shandong University, Qingdao 266237, China*

Complete contact information is available at:
https://pubs.acs.org/10.1021/acscatal.2c04292

Notes

The authors declare no competing financial interest.

■ ACKNOWLEDGMENTS

■ REFERENCES

(1) (a) Bringmann, G.; Price Mortimer, A. J.; Keller, P. A.; Gresser, M. J.; Garner, J.; Breuning, M. Atroposelective Synthesis of Axially Chiral Biaryl Compounds. *Angew. Chem., Int. Ed.* **2005**, *44*, 5384−5427. (b) Kozlowski, M. C.; Morgan, B. J.; Linton, E. C. Total synthesis of chiral biaryl natural products by asymmetric biaryl coupling. *Chem. Soc. Rev.* **2009**, *38*, 3193−3207. (c) Clayden, J.; Moran, W. J.; Edwards, P. J.; LaPlante, S. R. The Challenge of Atropisomerism in Drug Discovery. *Angew. Chem., Int. Ed.* **2009**, *48*, 6398−6401. (d) Bringmann, G.; Gulder, T.; Gulder, T. A. M.; Breuning, M. Atroposelective Total Synthesis of Axially Chiral Biaryl Natural Products. *Chem. Rev.* **2011**, *111*, 563−639. (e) Wencel-Delord, J.; Panossian, A.; Leroux, F. R.; Colobert, F. Recent Advances and New Concepts for the Synthesis of Axially Stereoenriched Biaryls. *Chem. Soc. Rev.* **2015**, *44*, 3418−3430. (f) Carmona, J. A.; Rodríguez-Franco, C.; Fernández, R.; Hornillos, V.; Lassaletta, J. M. Atroposelective transformation of axially chiral (hetero)biaryls. From desymmetrization to modern resolution strategies. *Chem. Soc. Rev.* **2021**, *50*, 2968−2983.

(2) (a) Chen, X.; Engle, K. M.; Wang, D.-H.; Yu, J.-Q. Palladium(II)-Catalyzed C-H Activation/C-C Cross-Coupling Reactions: Versatility and Practicality. *Angew. Chem., Int. Ed.* **2009**, *48*, 5094−5115. (b) Ye, J.; Lautens, M. Palladium-Catalysed Norbornene-Mediated C−H Functionalization of Arenes. *Nat. Chem.* **2015**, *7*, 863−870. (c) Shao, Q.; Wu, K.; Zhuang, Z.; Qian, S.; Yu, J.-Q. From Pd(OAc)$_2$ to Chiral Catalysts: The Discovery and Development of Bifunctional Mono-N-Protected Amino Acid Ligands for Diverse C−H Functionalization Reactions. *Acc. Chem. Res.* **2020**, *53*, 833−851. (d) Wang, P.-S.; Gong, L.-Z. Palladium Catalyzed Asymmetric Allylic C−H Functionalization: Mechanism, Stereo- and Regioselectivities, and Synthetic Applications. *Acc. Chem. Res.* **2020**, *53*, 2841−2854.

(e) Liao, G.; Zhang, T.; Lin, Z.-K.; Shi, B.-F. Transition Metal-Catalyzed Enantioselective C−H Functionalization via Chiral Transient Directing Group Strategies. *Angew. Chem., Int. Ed.* **2020**, *59*, 19773−19786. (f) Kitagawa, O. Chiral Pd-Catalyzed Enantioselective Syntheses of Various N−C Axially Chiral Compounds and Their Synthetic Applications. *Acc. Chem. Res.* **2021**, *54*, 719−730.

(3) (a) Ros, A.; López-Rodríguez, R.; Estepa, B.; Álvarez, E.; Fernández, R.; Lassaletta, J. M. Hydrazone as the Directing Group for Ir-Catalyzed Arene Diborylations and Sequential Functionalizations. *J. Am. Chem. Soc.* **2012**, *134*, 4573−4576. (b) Ye, B.; Cramer, N. Chiral Cyclopentadienyls: Enabling Ligands for Asymmetric Rh(III)-Catalyzed C−H Functionalizations. *Acc. Chem. Res.* **2015**, *48*, 1308−1318. (c) Hethcox, J. C.; Shockley, S. E.; Stoltz, B. M. Iridium-Catalyzed Diastereo-, Enantio-, and Regioselective Allylic Alkylation with Prochiral Enolates. *ACS Catal.* **2016**, *6*, 6207−6213. (d) Woźniak, Ł.; Tan, J.-F.; Nguyen, Q.-H.; Madron du Vigné, A.; Smal, V.; Cao, Y.-X.; Cramer, N. Catalytic Enantioselective Functionalizations of C−H Bonds by Chiral Iridium Complexes. *Chem. Rev.* **2020**, *120*, 10516−10543. (e) Shaaban, S.; Davies, C.; Waldmann, H. Applications of Chiral Cyclopentadienyl (Cp^x) Metal Complexes in Asymmetric Catalysis. *Eur. J. Org. Chem.* **2020**, *2020*, 6512−6524. (f) Romero-Arenas, A.; Hornillos, V.; Iglesias-Sigüenza, J.; Fernández, R.; López-Serrano, J.; Ros, A.; Lassaletta, J. M. Ir-Catalyzed Atroposelective Desymmetrization of Heterobiaryls: Hydroarylation of Vinyl Ethers and Bicycloalkenes. *J. Am. Chem. Soc.* **2020**, *142*, 2628−2639. (g) Yoshino, T.; Satake, S.; Matsunaga, S. Diverse Approaches for Enantioselective C−H Functionalization Reactions Using Group 9 Cp^{x}M^{III} Catalysts. *Chem. − Eur. J.* **2020**, *26*, 7346−7357. (h) Mas-Roselló, J.; Herraiz, A. G.; Audic, B.; Laverny, A.; Cramer, N. Chiral Cyclopentadienyl Ligands: Design, Syntheses, and Applications in Asymmetric Catalysis. *Angew. Chem., Int. Ed.* **2021**, *60*, 13198−13224. (i) Jacob, N.; Zaid, Y.; Oliveira, J. C. A.; Ackermann, L.; Wencel-Delord, J. Cobalt-Catalyzed Enantioselective C−H Arylation of Indoles. *J. Am. Chem. Soc.* **2022**, *144*, 798−806.

(4) (a) Kaga, A.; Chiba, S. Engaging Radicals in Transition Metal Catalyzed Cross-Coupling with Alkyl Electrophiles: Recent Advances. *ACS Catal.* **2017**, *7*, 4697−4706. (b) Loup, J.; Dhawa, U.; Pesciaioli, F.; Wencel-Delord, J.; Ackermann, L. Enantioselective C−H Activation with Earth-Abundant 3d Transition Metals. *Angew. Chem., Int. Ed.* **2019**, *58*, 12803−12818. (c) Diesel, J.; Cramer, N. Modular Chiral N-Heterocyclic Carbene Ligands for the Nickel-Catalyzed Enantioselective C−H Functionalization of Heterocycles. *Chimia* **2020**, *74*, 278−284. (d) Chen, H.; Wang, Y.-X.; Luan, Y.-X.; Ye, M. Enantioselective Twofold C−H Annulation of Formamides and Alkynes without Built-in Chelating Groups. *Angew. Chem., Int. Ed.* **2020**, *59*, 9428−9432.

(5) For selected reviews, see: (a) Newton, C. G.; Wang, S.-G.; Oliveira, C. C.; Cramer, N. Catalytic Enantioselective Transformations Involving C−H Bond Cleavage by Transition-Metal Complexes. *Chem. Rev.* **2017**, *117*, 8908−8976. (b) Liao, G.; Zhou, T.; Yao, Q.-J.; Shi, B.-F. Recent advances in the synthesis of axially chiral biaryls via transition metal-catalysed asymmetric C−H functionalization. *Chem. Commun.* **2019**, *55*, 8514−8523. (c) Achar, T. K.; Maiti, S.; Jana, S.; Maiti, D. Transition Metal Catalyzed Enantioselective C(sp^2)−H Bond Functionalization. *ACS Catal.* **2020**, *10*, 13748−13793. (d) Liu, C.-X.; Zhang, W.-W.; Yin, S.-Y.; Gu, Q.; You, S.-L. Synthesis of Atropisomers by Transition-Metal-Catalyzed Asymmetric C−H Functionalization Reactions. *J. Am. Chem. Soc.* **2021**, *143*, 14025−14040. (e) Cheng, J. K.; Xiang, S.-H.; Li, S.; Ye, L.; Tan, B. Recent Advances in Catalytic Asymmetric Construction of Atropisomers. *Chem. Rev.* **2021**, *121*, 4805−4902. (f) Zhang, X.; Zhao, K.; Gu, Z. Transition Metal-Catalyzed Biaryl Atropisomer Synthesis via a Torsional Strain Promoted Ring-Opening Reaction. *Acc. Chem. Res.* **2022**, *55*, 1620−1633. (g) Yue, Q.; Liu, B.; Liao, G.; Shi, B.-F. Binaphthyl Scaffold: A Class of Versatile Structure in Asymmetric C−H Functionalization. *ACS Catal.* **2022**, *12*, 9359−9396. (h) Zhang, Q.; Wu, L.-S.; Shi, B.-F. Forging C−heteroatom bonds by transition-metal-catalyzed enantioselective C−H functionalization. *Chem* **2022**, *8*, 384−413. (i) Zhang, Z.-X.; Zhai, T.-Y.; Ye,

L.-W. Synthesis of axially chiral compounds through catalytic asymmetric reactions of alkynes. *Chem. Catal.* **2021**, *1*, 1378−1412. (j) Mei, G.-J.; Wong, J. J.; Zheng, W.; Nangia, A. A.; Houk, K. N.; Lu, Y. Rational design and atroposelective synthesis of N−N axially chiral compounds. *Chem* **2021**, *7*, 2743−2757. For selected examples, see: (k) Teng, F.; Yu, T.; Peng, Y.; Hu, W.; Hu, H.; He, Y.; Luo, S.; Zhu, Q. Palladium-Catalyzed Atroposelective Coupling−Cyclization of 2-Isocyanobenzamides to Construct Axially Chiral 2-Aryl- and 2,3-Diarylquinazolinones. *J. Am. Chem. Soc.* **2021**, *143*, 2722−2728. (l) Liao, G.; Zhang, T.; Jin, L.; Wang, B.-J.; Xu, C.-K.; Lan, Y.; Zhao, Y.; Shi, B.-F. Experimental and Computational Studies on the Directing Ability of Chalcogenoethers in Palladium-Catalyzed Atroposelective C−H Olefination and Allylation. *Angew. Chem., Int. Ed.* **2022**, *61*, No. e202115221. (m) Guo, W.-T.; Zhu, B.-H.; Chen, Y.; Yang, J.; Qian, P.-C.; Deng, C.; Ye, L.-W.; Li, L. Enantioselective Rh-Catalyzed Azide-Internal-Alkyne Cycloaddition for the Construction of Axially Chiral 1,2,3-Triazoles. *J. Am. Chem. Soc.* **2022**, *144*, 6981−6991. (n) Mei, G.-J.; Koay, W. L.; Guan, C.-Y.; Lu, Y. Atropisomers beyond the C−C axial chirality: Advances in catalytic asymmetric synthesis. *Chem* **2022**, *8*, 1855−1893. (o) Guo, Y.; Liu, M.-M.; Zhu, X.; Zhu, L.; He, C. Catalytic Asymmetric Synthesis of Silicon-Stereogenic Dihydrodibenzosilines: Silicon Central-to-Axial Chirality Relay. *Angew. Chem., Int. Ed.* **2021**, *60*, 13887−13891. (p) Xu, Q.; Zhang, H.; Ge, F.-B.; Wang, X.-M.; Zhang, P.; Lu, C.-J.; Liu, R.-R. Cu(I)-Catalyzed Asymmetric Arylation of Pyrroles with Diaryliodonium Salts toward the Synthesis of N−N Atropisomers. *Org. Lett.* **2022**, *24*, 3138−3143.

(6) (a) Ye, B.; Cramer, N. Chiral Cyclopentadienyl Ligands as Stereocontrolling Element in Asymmetric C-H Functionalization. *Science* **2012**, *338*, 504−506. (b) Ye, B.; Cramer, N.; Tunable, A. Class of Chiral Cp Ligands for Enantioselective Rhodium(III)-Catalyzed C−H Allylations of Benzamides. *J. Am. Chem. Soc.* **2013**, *135*, 636−639. (c) Sun, Y.; Cramer, N. Tailored trisubstituted chiral CpˣRhIII catalysts for kinetic resolutions of phosphinic amides. *Chem. Sci.* **2018**, *9*, 2981−2985. (d) Duchemin, C.; Smits, G.; Cramer, N. RhI, IrIII,and CoIII Complexes with Atropchiral Biaryl Cyclopentadienyl Ligands: Syntheses, Structures, and Catalytic Activities. *Organometallics* **2019**, *38*, 3939−3947. (e) Sun, Y.; Cramer, N. Rhodium(III)-Catalyzed Enantiotopic C−H Activation Enables Access to *P*-Chiral Cyclic Phosphinamides. *Angew. Chem., Int. Ed.* **2017**, *56*, 364−367. (f) Wang, S.-G.; Liu, Y.; Cramer, N. Asymmetric Alkenyl C−H Functionalization by CpxRhIII forms 2H-Pyrrol-2-ones through [4+1]-Annulation of Acryl Amides and Allenes. *Angew. Chem., Int. Ed.* **2019**, *58*, 18136−18140. (g) Duchemin, C.; Cramer, N. Chiral cyclopentadienyl RhIII-catalyzed enantioselective cyclo-propanation of electron-deficient olefins enable rapid access to UPF-648 and oxylipin natural products. *Chem. Sci.* **2019**, *10*, 2773−2777. (h) Wang, S.-G.; Cramer, N. Asymmetric CpxRh(III)-Catalyzed Acrylic Acid C−H Functionalization with Allenes Provides Chiral γ-Lactones. *ACS Catal.* **2020**, *10*, 8231−8236. (i) Duchemin, C.; Cramer, N. Enantioselective CpˣRhIII-Catalyzed Carboaminations of Acrylates. *Angew. Chem., Int. Ed.* **2020**, *59*, 14129−14133.

(7) (a) Zheng, J.; Cui, W.-J.; Zheng, C.; You, S.-L. Synthesis and Application of Chiral Spiro Cp Ligands in Rhodium-Catalyzed Asymmetric Oxidative Coupling of Biaryl Compounds with Alkenes. *J. Am. Chem. Soc.* **2016**, *138*, 5242−5245. (b) Cui, W.-J.; Wu, Z.-J.; Gu, Q.; You, S.-L. Divergent Synthesis of Tunable Cyclopentadienyl Ligands and Their Application in Rh-Catalyzed Enantioselective Synthesis of Isoindolinone. *J. Am. Chem. Soc.* **2020**, *142*, 7379−7385.

(8) (a) Jia, Z.-J.; Merten, C.; Gontla, R.; Daniliuc, C. G.; Antonchick, A. P.; Waldmann, H. General Enantioselective C−H Activation with Efficiently Tunable Cyclopentadienyl Ligands. *Angew. Chem., Int. Ed.* **2017**, *56*, 2429−2434. (b) Pan, C.; Yin, S.-Y.; Wang, S.-B.; Gu, Q.; You, S.-L. Oxygen-Linked Cyclopentadienyl Rhodium-(III) Complexes-Catalyzed Asymmetric C−H Arylation of Benzo[h]-quinolines with 1-Diazonaphthoquinones. *Angew. Chem., Int. Ed.* **2021**, *60*, 15510−15516.

(9) Trifonova, E. A.; Ankudinov, N. M.; Mikhaylov, A. A.; Chusov, D. A.; Nelyubina, Y. V.; Perekalin, D. S. A Planar-Chiral Rhodium-(III) Catalyst with a Sterically Demanding Cyclopentadienyl Ligand and Its Application in the Enantioselective Synthesis of Dihydroiso-quinolones. *Angew. Chem., Int. Ed.* **2018**, *57*, 7714−7718.

(10) (a) Liang, H.; Vasamsetty, L.; Li, T.; Jiang, J.; Pang, X.; Wang, J. A New Class of C2-Symmetric Chiral Cyclopentadienyl Ligand Derived from Ferrocene Scaffold: Design, Synthesis and Application. *Chem. − Eur. J.* **2020**, *26*, 14546−14550. (b) Li, G.; Yan, X.; Jiang, J.; Liang, H.; Zhou, C.; Wang, J. Chiral Bicyclo[2.2.2]octane-Fused CpRh Complexes: Synthesis and Potential Use in Asymmetric C−H Activation. *Angew. Chem., Int. Ed.* **2020**, *59*, 22436−22440. (c) Yan, X.; Jiang, J.; Wang, J. A Class of Readily Tunable Planar-Chiral Cyclopentadienyl Rhodium(III) Catalysts for Asymmetric C−H Activation. *Angew. Chem., Int. Ed.* **2022**, *61*, No. e202201522.

(11) (a) Hyster, T. K.; Knörr, L.; Ward, T. R.; Rovis, T. Biotinylated Rh(III) Complexes in Engineered Streptavidin for Accelerated Asymmetric C-H Activation. *Science* **2012**, *338*, 500−503. (b) Tian, M.; Bai, D.; Zheng, G.; Chang, J.; Li, X. Rh(III)-Catalyzed Asymmetric Synthesis of Axially Chiral Biindolyls by Merging C−H Activation and Nucleophilic Cyclization. *J. Am. Chem. Soc.* **2019**, *141*, 9527−9532. (c) Mi, R.; Zheng, G.; Qi, Z.; Li, X. Rhodium-Catalyzed Enantioselective Oxidative [3+2] Annulation of Arenes and Azabicyclic Olefins through Twofold C−H Activation. *Angew. Chem., Int. Ed.* **2019**, *58*, 17666−17670. (d) Wang, F.; Qi, Z.; Zhao, Y.; Zhai, S.; Zheng, G.; Mi, R.; Huang, Z.; Zhu, X.; He, X.; Li, X. Rhodium(III)-Catalyzed Atroposelective Synthesis of Biaryls by C−H Activation and Intermolecular Coupling with Sterically Hindered Alkynes. *Angew. Chem., Int. Ed.* **2020**, *59*, 13288−13294. (e) Zheng, G.; Zhou, Z.; Zhu, G.; Zhai, S.; Xu, H.; Duan, X.; Yi, W.; Li, X. Rhodium(III)-Catalyzed Enantio- and Diastereoselective C−H Cyclopropylation of N-Phenoxylsulfonamides: Combined Experimen-tal and Computational Studies. *Angew. Chem., Int. Ed.* **2020**, *59*, 2890−2896. (f) Wang, J.; Chen, H.; Kong, L.; Wang, F.; Lan, Y.; Li, X. Enantioselective and Diastereoselective C−H Alkylation of Benzamides: Synergized Axial and Central Chirality via a Single Stereodetermining Step. *ACS Catal.* **2021**, *11*, 9151−9158. (g) Wang, F.; Jing, J.; Zhao, Y.; Zhu, X.; Zhang, X.-P.; Zhao, L.; Hu, P.; Deng, W.-Q.; Li, X.; Rhodium-Catalyzed, C−H. Activation-Based Con-struction of Axially and Centrally Chiral Indenes through Two Discrete Insertions. *Angew. Chem., Int. Ed.* **2021**, *60*, 16628−16633. (h) Hu, P.; Kong, L.; Wang, F.; Zhu, X.; Li, X.; Twofold, C−H. Activation-Based Enantio- and Diastereoselective C−H Arylation Using Diarylacetylenes as Rare Arylating Reagents. *Angew. Chem., Int. Ed.* **2021**, *60*, 20424−20429. (i) Mi, R.; Chen, H.; Zhou, X.; Li, N.; Ji, D.; Wang, F.; Lan, Y.; Li, X. Rhodium-Catalyzed Atroposelective Access to Axially Chiral Olefins via C−H Bond Activation and Directing Group Migration. *Angew. Chem., Int. Ed.* **2022**, *61*, No. e202111860.

(12) (a) Dieckmann, M.; Jang, Y.-S.; Cramer, N. Chiral Cyclo-pentadienyl Iridium(III) Complexes Promote Enantioselective Cyclo-isomerizations Giving Fused Cyclopropanes. *Angew. Chem., Int. Ed.* **2015**, *54*, 12149−12152. (b) Jang, Y.-S.; Dieckmann, M.; Cramer, N. Cooperative Effects between Chiral Cpˣ−Iridium(III) Catalysts and Chiral Carboxylic Acids in Enantioselective C−H Amidations of Phosphine Oxides. *Angew. Chem., Int. Ed.* **2017**, *56*, 15088−15092. (c) Woźniak, Ł.; Cramer, N. Atropo-Enantioselective Oxidation-Enabled Iridium(III)-Catalyzed C−H Arylations with Aryl Boronic Esters. *Angew. Chem., Int. Ed.* **2021**, *60*, 18532−18536.

(13) (a) Ozols, K.; Jang, Y.-S.; Cramer, N. Chiral Cyclopentadienyl Cobalt(III) Complexes Enable Highly Enantioselective 3d-Metal-Catalyzed C−H Functionalizations. *J. Am. Chem. Soc.* **2019**, *141*, 5675−5680. (b) Ozols, K.; Onodera, S.; Woźniak, Ł.; Cramer, N. Cobalt(III)-Catalyzed Enantioselective Intermolecular Carboamina-tion by C−H Functionalization. *Angew. Chem., Int. Ed.* **2021**, *60*, 655−659.

(14) Liang, H.; Guo, W.; Li, J.; Jiang, J.; Wang, J. Chiral Arene Ligand as Stereocontroller for Asymmetric C−H Activation. *Angew. Chem., Int. Ed.* **2022**, *61*, No. e202204926.

(15) Alternatively, in achiral transition-metal/chiral acid-catalyzed enantioselective C−H activation systems, the linear chirality transfer

discussed in Scheme 1a is not relevant since the enantio-determining proto-demetalation step simply controls the stereochemistry without chirality transfer from intermediates. See: (a) Pesciaioli, F.; Dhawa, U.; Oliveira, J. C. A.; Yin, R.; John, M.; Ackermann, L. Enantioselective Cobalt(III)-Catalyzed C−H Activation Enabled by Chiral Carboxylic Acid Cooperation. *Angew. Chem., Int. Ed.* **2018**, *57*, 15425−15429. (b) Satake, S.; Kurihara, T.; Nishikawa, K.; Mochizuki, T.; Hatano, M.; Ishihara, K.; Yoshino, T.; Matsunaga, S. Pentamethylcyclopentadienyl rhodium(III)−chiral disulfonate hybrid catalysis for enantioselective C−H bond functionalization. *Nat. Catal.* **2018**, *1*, 585−591. (c) Kurihara, T.; Kojima, M.; Yoshino, T.; Matsunaga, S. Cp*CoIII/Chiral Carboxylic Acid-Catalyzed Enantioselective 1,4-Addition Reactions of Indoles to Maleimides. *Asian J. Org. Chem.* **2020**, *9*, 368−371. (d) Dhawa, U.; Connon, R.; Oliveira, J. C. A.; Steinbock, R.; Ackermann, L. Enantioselective Ruthenium-Catalyzed C−H Alkylations by a Chiral Carboxylic Acid with Attractive Dispersive Interactions. *Org. Lett.* **2021**, *23*, 2760−2765.

(16) Wang, S.-G.; Cramer, N. An Enantioselective Cp^XRh(III)-Catalyzed C-H Functionalization/Ring-Opening Route to Chiral Cyclopentenylamines. *Angew. Chem., Int. Ed.* **2019**, *58*, 2514−2518.

(17) Jang, Y.-S.; Woźniak, Ł.; Pedroni, J.; Cramer, N. Access to P- and Axially Chiral Biaryl Phosphine Oxides by Enantioselective Cp^xIrIII-Catalyzed C−H Arylations. *Angew. Chem., Int. Ed.* **2018**, *57*, 12901−12905.

(18) Selected chirality transfer in non-C−H activation systems: (a) Guo, F.; Konkol, L. C.; Thomson, R. J. Enantioselective Synthesis of Biphenols from 1,4-Diketones by Traceless Central-to-Axial Chirality Exchange. *J. Am. Chem. Soc.* **2011**, *133*, 18−20. (b) Link, A.; Sparr, C. Organocatalytic Atroposelective Aldol Condensation: Synthesis of Axially Chiral Biaryls by Arene Formation. *Angew. Chem., Int. Ed.* **2014**, *53*, 5458−5461. (c) Raut, V. S.; Jean, M.; Vanthuyne, N.; Roussel, C.; Constantieux, T.; Bressy, C.; Bugaut, X.; Bonne, D.; Rodriguez, J. Enantioselective Syntheses of Furan Atropisomers by an Oxidative Central-to-Axial Chirality Conversion Strategy. *J. Am. Chem. Soc.* **2017**, *139*, 2140−2143. (d) Xu, K.; Li, W.; Zhu, S.; Zhu, T. Atroposelective Arene Formation by Carbene-Catalyzed Formal [4+2] Cycloaddition. *Angew. Chem., Int. Ed.* **2019**, *58*, 17625−17630. (e) Hu, Y.-L.; Wang, Z.; Yang, H.; Chen, J.; Wu, Z.-B.; Lei, Y.; Zhou, L. Conversion of two stereocenters to one or two chiral axes: atroposelective synthesis of 2,3-diarylbenzoindoles. *Chem. Sci.* **2019**, *10*, 6777−6784. (f) Wu, X.; Sparr, C. Stereoselective Synthesis of Atropisomeric Acridinium Salts by the Catalyst-Controlled Cyclization of ortho-Quinone Methide Iminiums. *Angew. Chem., Int. Ed.* **2022**, *61*, No. e202201424. (g) An, Q.-J.; Xia, W.; Ding, W.-Y.; Liu, H.-H.; Xiang, S.-H.; Wang, Y.-B.; Zhong, G.; Tan, B. Nitrosobenzene-Enabled Chiral Phosphoric Acid Catalyzed Enantioselective Construction of Atropisomeric N-Arylbenzimidazoles. *Angew. Chem., Int. Ed.* **2021**, *60*, 24888−24893.

(19) (a) Wu, S.; Huang, X.; Wu, W.; Li, P.; Fu, C.; Ma, S. A C-H bond activation-based catalytic approach to tetrasubstituted chiral allenes. *Nat. Commun.* **2015**, *6*, No. 7946. (b) Lu, Q.; Greßies, S.; Klauck, F. J. R.; Glorius, F. Manganese(I)-Catalyzed Regioselective C−H Allenylation: Direct Access to 2-Allenylindoles. *Angew. Chem., Int. Ed.* **2017**, *56*, 6660−6664. (c) Mao, R.; Zhao, Y.; Zhu, X.; Wang, F.; Deng, W.-Q.; Li, X. Rhodium-Catalyzed and Chiral Zinc Carboxylate-Assisted Allenylation of Benzamides via Kinetic Resolution. *Org. Lett.* **2021**, *23*, 7038−7043.

(20) Dong, K.; Fan, X.; Pei, C.; Zheng, Y.; Chang, S.; Cai, J.; Qiu, L.; Yu, Z.-X.; Xu, X. Transient-axial-chirality controlled asymmetric rhodium-carbene C(sp2)-H functionalization for the synthesis of chiral fluorenes. *Nat. Commun.* **2020**, *11*, No. 2363.

(21) (a) Li, S.-X.; Ma, Y.-N.; Yang, S.-D. P(O)R2-Directed Enantioselective C−H Olefination toward Chiral Atropoisomeric Phosphine−Olefin Compounds. *Org. Lett.* **2017**, *19*, 1842−1845. (b) Yan, X.; Zhao, P.; Liang, H.; Xie, H.; Jiang, J.; Gou, S.; Wang, J. Rhodium(III)-Catalyzed Asymmetric C−H Activation of N-Methoxybenzamide with Quinone and Its Application in the Asymmetric Synthesis of a Dihydrolycoricidine Analogue. *Org. Lett.* **2020**, *22*, 3219−3223.

(22) (a) Nagata, T.; Satoh, T.; Nishii, Y.; Miura, M. Rhodium-Catalyzed Oxidative Annulation of (2-Arylphenyl)boronic Acids with Alkynes: Selective Synthesis of Phenanthrene Derivatives. *Synlett* **2016**, *27*, 1707−1710. (b) Xu, S.; Huang, B.; Qiao, G.; Huang, Z.; Zhang, Z.; Li, Z.; Wang, P.; Zhang, Z. Rh(III)-Catalyzed C−H Activation of Boronic Acid with Aryl Azide. *Org. Lett.* **2018**, *20*, 5578−5582. (c) Liu, B.; Yang, L.; Dong, Z.; Chang, J.; Li, X. Rh(III)-Catalyzed Annulation of 2-Biphenylboronic Acid with Diverse Activated Alkenes. *Org. Lett.* **2021**, *23*, 7199−7204.

(23) (a) Chan, W.-W.; Lo, S.-F.; Zhou, Z.; Yu, W.-Y. Rh-Catalyzed Intermolecular Carbenoid Functionalization of Aromatic C−H Bonds by α-Diazomalonates. *J. Am. Chem. Soc.* **2012**, *134*, 13565−13568. (b) Shi, Z.; Koester, D. C.; Boultadakis-Arapinis, M.; Glorius, F. Rh(III)-Catalyzed Synthesis of Multisubstituted Isoquinoline and Pyridine N-Oxides from Oximes and Diazo Compounds. *J. Am. Chem. Soc.* **2013**, *135*, 12204−12207. (c) Tan, W. W.; Yoshikai, N. Copper-catalyzed condensation of imines and α-diazo-β-dicarbonyl compounds: modular and regiocontrolled synthesis of multisubstituted pyrroles. *Chem. Sci.* **2015**, *6*, 6448−6455. (d) Yang, Y.; Wang, X.; Li, Y.; Zhou, B. A [4+1] Cyclative Capture Approach to 3H-Indole-N-oxides at Room Temperature by Rhodium(III)-Catalyzed C−H Activation. *Angew. Chem., Int. Ed.* **2015**, *54*, 15400−15404. (e) Feng, J.; Li, B.; He, Y.; Gu, Z. Enantioselective Synthesis of Atropisomeric Vinyl Arene Compounds by Palladium Catalysis: A Carbene Strategy. *Angew. Chem., Int. Ed.* **2016**, *55*, 2186−2190. (f) Biswas, A.; Pan, S.; Samanta, R. Cu(II)-Catalyzed Construction of Heterobiaryls using 1-Diazonaphthoquinones: A General Strategy for the Synthesis of QUINOX and Related P,N Ligands. *Org. Lett.* **2022**, *24*, 1631−1636. (g) Kattela, S.; Roque, D.; Correia, C.; Hornillos, V.; Iglesias-Sigüenza, J.; Fernández, R.; Lassaletta, J. M. Pd-Catalyzed Dynamic Kinetic Asymmetric Cross-Coupling of Heterobiaryl Bromides with N-Tosylhydrazones. *Org. Lett.* **2022**, *24*, 3812−3816.

(24) (a) Fang, Z.-J.; Zheng, S.-C.; Guo, Z.; Guo, J.-Y.; Tan, B.; Liu, X.-Y. Asymmetric Synthesis of Axially Chiral Isoquinolones: Nickel-Catalyzed Denitrogenative Transannulation. *Angew. Chem., Int. Ed.* **2015**, *54*, 9528−9532. (b) Jia, S.; Li, S.; Liu, Y.; Qin, W.; Yan, H. Enantioselective Control of Both Helical and Axial Stereogenic Elements though an Organocatalytic Approach. *Angew. Chem., Int. Ed.* **2019**, *58*, 18496−18501. (c) Peng, L.; Li, K.; Xie, C.; Li, S.; Xu, D.; Qin, W.; Yan, H. Organocatalytic Asymmetric Annulation of ortho-Alkynylanilines: Synthesis of Axially Chiral Naphthyl-C2-indoles. *Angew. Chem., Int. Ed.* **2019**, *58*, 17199−17204. (d) Xu, M.-M.; You, X.-Y.; Zhang, Y.-Z.; Lu, Y.; Tan, K.; Yang, L.; Cai, Q. Enantioselective Synthesis of Axially Chiral Biaryls by Diels−Alder/Retro-Diels−Alder Reaction of 2-Pyrones with Alkynes. *J. Am. Chem. Soc.* **2021**, *143*, 8993−9001. (e) Jia, S.; Tian, Y.; Li, X.; Wang, P.; Lan, Y.; Yan, H. Atroposelective Construction of Nine-Membered Carbonate-Bridged Biaryls. *Angew. Chem., Int. Ed.* **2022**, *134*, No. e202206501.

(25) (a) Shibata, T.; Nishizawa, G.; Endo, K. Iridium-Catalyzed Enantioselective Formal [4+2] Cycloaddition of Biphenylene and Alkynes for the Construction of Axial Chirality. *Synlett* **2008**, *2008*, 765−768. (b) Farr, C. M. B.; Kazerouni, A. M.; Park, B.; Poff, C. D.; Won, J.; Sharp, K. R.; Baik, M.-H.; Blakey, S. B. Designing a Planar Chiral Rhodium Indenyl Catalyst for Regio- and Enantioselective Allylic C−H Amidation. *J. Am. Chem. Soc.* **2020**, *142*, 13996−14004. (c) Takano, H.; Shiozawa, N.; Imai, Y.; Kanyiva, K. S.; Shibata, T. Catalytic Enantioselective Synthesis of Axially Chiral Polycyclic Aromatic Hydrocarbons (PAHs) via Regioselective C−C Bond Activation of Biphenylenes. *J. Am. Chem. Soc.* **2020**, *142*, 4714−4722.

(26) (a) Ford, W. T.; Thompson, T. B.; Snoble, K. A. J.; Timko, J. M. Hindered rotation in 9-arylfluorenes. Resolutions of the mechanistic question. *J. Am. Chem. Soc.* **1975**, *97*, 95−101. (b) Li, S.-G.; Wang, Y.-T.; Zhang, Q.; Wang, K.-B.; Xue, J.-J.; Li, D.-H.; Jing, Y.-K.; Lin, B.; Hua, H.-M. Pegaharmols A−B, Axially Chiral β-Carboline-quinazoline Dimers from the Roots of Peganum harmala. *Org. Lett.* **2020**, *22*, 7522−7525. (c) Bertuzzi, G.; Corti, V.; Izzo, J. A.; Ričko, S.; Jessen, N. I.; Jørgensen, K. A. Organocatalytic Enantioselective Construction of Conformationally Stable C(sp2)−C(sp3) Atropisomers. *J. Am. Chem. Soc.* **2022**, *144*, 1056−1065.

(27) (a) Huo, H.; Gorsline, B. J.; Fu, G. C. Catalyst-controlled doubly enantioconvergent coupling of racemic alkyl nucleophiles and electrophiles. *Science* **2020**, *367*, 559−564. (b) Yang, Z.-P.; Freas, D. J.; Fu, G. C. The Asymmetric Synthesis of Amines via Nickel-Catalyzed Enantioconvergent Substitution Reactions. *J. Am. Chem. Soc.* **2021**, *143*, 2930−2937. (c) Yang, Z.-P.; Freas, D. J.; Fu, G. C. Asymmetric Synthesis of Protected Unnatural α-Amino Acids via Enantioconvergent Nickel-Catalyzed Cross-Coupling. *J. Am. Chem. Soc.* **2021**, *143*, 8614−8618. (d) Wang, Z.; Yang, Z.-P.; Fu, G. C. Quaternary stereocentres via catalytic enantioconvergent nucleophilic substitution reactions of tertiary alkyl halides. *Nat. Chem.* **2021**, *13*, 236−242. (e) Poremba, K. E.; Kadunce, N. T.; Suzuki, N.; Cherney, A. H.; Reisman, S. E. Nickel-Catalyzed Asymmetric Reductive Cross-Coupling to Access 1,1-Diarylalkanes. *J. Am. Chem. Soc.* **2017**, *139*, 5684−5687.

(28) Audic, B.; Wodrich, M. D.; Cramer, N. Mild complexation protocol for chiral Cp^{x}Rh and Ir complexes suitable for in situ catalysis. *Chem. Sci.* **2019**, *10*, 781−787.

(29) For asymmetric C-H activation using diazo reagents, see: (a) Xiao, Q.; Xia, Y.; Li, H.; Zhang, Y.; Wang, J. Coupling of *N*-Tosylhydrazones with Terminal Alkynes Catalyzed by Copper(I): Synthesis of Trisubstituted Allenes. *Angew. Chem., Int. Ed.* **2011**, *50*, 1114−1117. (b) Ye, B.; Cramer, N. Asymmetric Synthesis of Isoindolones by Chiral Cyclopentadienyl-Rhodium(III)-Catalyzed C-H Functionalizations. *Angew. Chem. Int. Ed* **2014**, *53*, 7896−7899. (c) Chen, X.; Yang, S.; Li, H.; Wang, B.; Song, G. Enantioselective C−H Annulation of Indoles with Diazo Compounds through a Chiral Rh(III) Catalyst. *ACS Catal.* **2017**, *7*, 2392−2396. (d) Sun, L.; Liu, B.; Zhao, Y.; Chang, J.; Kong, L.; Wang, F.; Deng, W.-Q.; Li, X. Rhodium(iii)-catalyzed asymmetric [4+1] spiroannulations of O-pivaloyl oximes with α-diazo compounds. *Chem. Commun.* **2021**, *57*, 8268−8271. For racemic reactions of diazo reagents, see ref 22.

(30) Fukagawa, S.; Kojima, M.; Yoshino, T.; Matsunaga, S. Catalytic Enantioselective Methylene C(sp^3)−H Amidation of 8-Alkylquinolines Using a Cp*Rh^{III}/Chiral Carboxylic Acid System. *Angew. Chem., Int. Ed.* **2019**, *58*, 18154−18158.

(31) Zhou, T.; Li, L.; Li, B.; Song, H.; Wang, B. Syntheses, Structures, and Reactions of Cyclometalated Rhodium, Iridium, and Ruthenium Complexes of *N*-Methoxy-4-nitrobenzamide. *Organometallics* **2018**, *37*, 476−481.

(32) Kohn, W.; Sham, L. J. Self-Consistent Equations Including Exchange and Correlation Effects. *Phys. Rev.* **1965**, *140*, A1133−A1138.

(33) Zheng, C.; Zheng, J.; You, S. A DFT Study on Rh-Catalyzed Asymmetric Dearomatization of 2-Naphthols Initiated with C-H Activation: A Refined Reaction Mechanism and Origins of Multiple Selectivity. *ACS Catal.* **2016**, *6*, 262−271.

(34) (a) Biggs, R. A.; Ogilvie, W. W. *Eliminations to Form Alkenes, Allenes, and Alkynes and Related Reactions*; Knochel, P., Ed.; Elsevier: Amsterdam, 2014; pp 802−841. (b) Mosconi, E.; De Angelis, F.; Belpassi, L.; Tarantelli, F.; Alunni, S. Merging of E2 and E1cb Reaction Mechanisms: A Combined Theoretical and Experimental Study. *Eur. J. Org. Chem.* **2009**, *2009*, 5501−5504.